Electronic Supplementary Material (ESI) for Lab on a Chip.

Supporting Information

Droplet Drinking in Constrictions

*Shi Feng, Chundong Xue, Cunliang Pan, Shengyang Tao**

S. Feng, Prof. S. Y. Tao

School of Chemistry, State Key Laboratory of Fine Chemicals, Frontier Science Center for Smart Materials, Dalian Key Laboratory of Intelligent Chemistry, Dalian University of Technology, Dalian 116024, China.

E-mail: taosy@dlut.edu.cn

C. D. Xue

School of Biomedical Engineering, Faculty of Medicine, Dalian University of Technology, Dalian 116024, P.R. China

C. L. Pan

Department of Engineering Mechanics, State Key Laboratory of Structural Analysis for Industrial Equipment, Dalian University of Technology, Dalian 116024, P.R. China

Index

1. Microfluidic device

Droplets are fabricated using a coaxial microfluidic device. The process for preparing a microfluidic chip to convert a single emulsion into a double emulsion proceeds as outlined below.

The microfluidic device consists of two cylindrical capillaries (inside diameter 0.58 mm and outside diameter 1.00 mm, WPI Inc., USA) aligned coaxially within a square capillary (orifice size: 1.05 mm × 1.05 mm, AIT Glass, USA). One of the cylindrical capillaries has a conical cross-section as shown in **Figure S1a**. Before assembling, the conical capillary is tapered to the orifice of 70 μm. Another cylindrical capillary with a constriction structure serves as the common outlet for all liquids. Transparent epoxy resin (5 Minute Epoxy, Devcon) is used to fix these capillaries on a glass slide (thickness: 1.0 mm, Guluoglass, P. R. China). At last, the exposed capillary wells are sealed using 3D-printed collectors for fluid injection.

If it is necessary to pre-generate a double emulsion and have it pass through constrictions, some modifications will be required in the preparation procedure of the microfluidic device (**Figure S1b**). The cylindrical capillaries with conical cross-section should be tapered to the orifice of 200 μm. When aiming to create a w/o/w-type double emulsion, the conical capillary tube needs to be treated with trimethoxy(octadecyl)silane to make it hydrophobic. The cylindrical capillary with a constriction does not require any special treatment. A small capillary (orifice size: 100 μm) is inserted in the conical capillary and kept at a distance from the exit of the

conical capillary. When attempting to prepare o/w/o-type double emulsions, both the conical capillary tube and the small capillary need to undergo oxygen-plasma treatment to make them hydrophilic.

For generating multi-core double emulsions, it is necessary to simultaneously create multiple constriction structures on the cylindrical capillary as shown in **Figure S1c**, and the number of constrictions matches the number of core droplets.

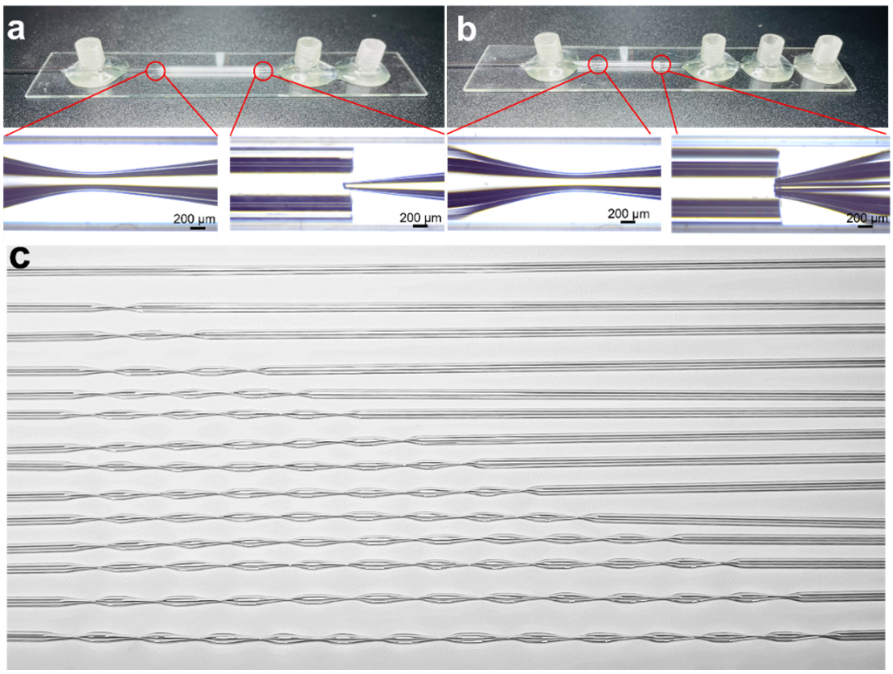

Supplementary Figure S1 (a) A microfluidic device used to pre-generate single emulsions in this study and microscopic photographs of constriction and capillary arrangement in the device. (b) A microfluidic device used to pre-generate double emulsions and microscopic images of constriction and capillary arrangement. (c) Image of glass capillaries with multiple constriction structures.

2. Geometric dimensions of the constriction

A capillary tube with a constriction structure can be characterized by several parameters, as illustrated in **Figure S2**. The inner radius of the straight section is denoted as R_{Tube}. while R_{Throat} represents the inner radius of the throat. The distance from the initial point of the constriction to the orifice is represented by D, a constant value across all capillaries. The total length of the constriction area is symbolized by L.

Within the constriction area, a Cartesian coordinate system is established, with the origin located at the geometric center of the narrowest part of the throat. This setup facilitates the depiction of the authentic geometric parameters of the constriction area. The sidewalls of the constriction channel can be succinctly represented by linear fitting, as illustrated in **Figure S3**

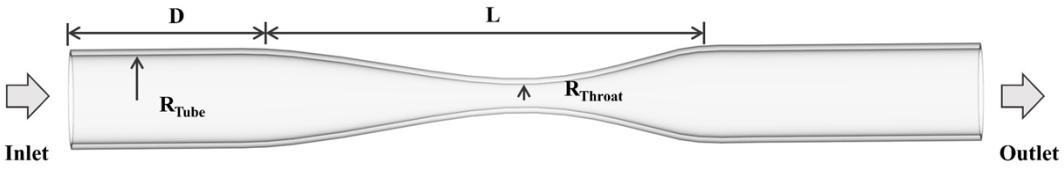

Supplementary Figure S2 A schematic diagram illustrating a capillary with constriction employed for the generation of double emulsions is provided.

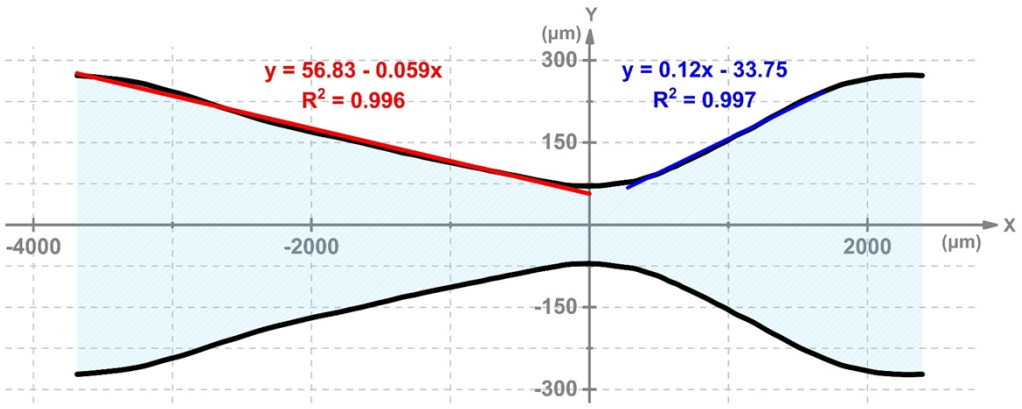

Supplementary Figure S3 A coordinate system is established to represent the authentic geometric parameters of the constriction. The inner radius of the throat (R_{Throat}) is measured at 70.83 μm.

A micropipette puller is deployed to generate constriction structures on capillaries. The program setting comprises 5 parameters. The HEAT setting impacts both the parameter L and R_{Throat}. The VELOCITY value indicates the speed at which the two puller bars move during the weak pull phase. A lower VELOCITY value corresponds to a slower bar speed when the throat is formed. The TIME parameter regulates the duration of cooling air activation. The PRESSURE setting governs the pressure of the cooling air supplied to the filament. Greater pressure results in a shorter taper. LOOP TIMES refers to the program's execution cycles, and the throat breaks at the 8th loop.

Supplementary Table S1. Program settings of the micropipette puller system and corresponding capillary geometry.

Cap.	Capillary geometry				Program settings				
	D (mm)	L (μm)	R_{Tube} (μm)	R_{throat} (μm)	Heat	Velocity	Time	Pressure	Loop times
1	35	4569	290	136.89	535	30	255	500	2
2	35	5107	290	108.06	535	30	255	500	3
3	35	5469	290	87.49	535	30	255	500	4
4	35	6080	290	70.83	535	30	255	500	5
5	35	6264	290	54.16	535	30	255	500	6
6	35	6481	290	41.66	535	30	255	500	7

3. Analysis of forces and flow field in droplet deformation

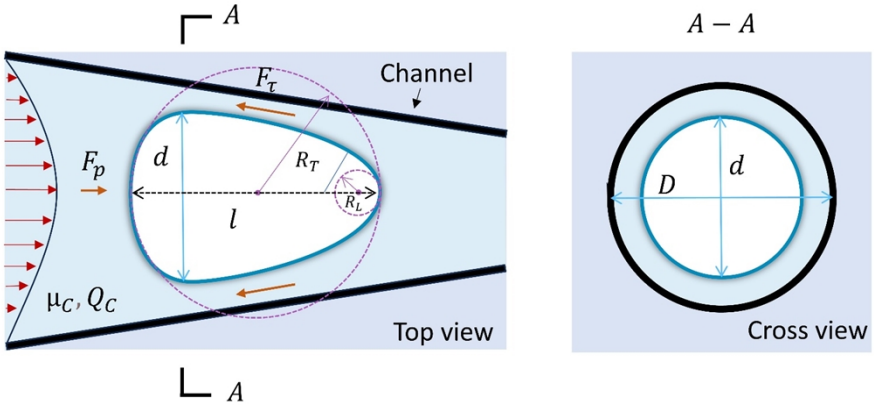

Supplementary Figure S4 A schematic illustration of the shape of the droplet in the upstream region of the constriction.

In the upstream region of the constriction, the shear force F_τ acting on the droplet and the pressure force F_p from the continuous phase can be determined by Newton's law of internal friction and the Hagen–Poiseuille equation, respectively.[1,2] Meanwhile,

the interfacial tension should be determined by the curvature radii of the liquid droplet's front and rear ends (as shown in **Figure S4**):

$$F_\tau = A_\tau \tau \approx 2\pi d \mu_c \int_0^l \tau(x) dx \#(1)$$

$$F_p = \Delta P A_{axial} \approx O\left(\frac{4\mu_C Q_C l d^2}{\pi\{(D-d)(D+d)\}^2}\right) \#(2)$$

$$F_\sigma \approx 2\sigma A_{axial}\left(\frac{1}{R_L} - \frac{1}{R_T}\right) \#(3)$$

μ_C represents the viscosity coefficient of the continuous phase, A_τ is the area of the primary friction surface of the liquid droplet, τ denotes the shear stress, l is the characteristic axial length of the primary friction surface of the droplet, d is the maximum radial diameter at the current position of the droplet, R_T and R_L are the curvature radii of the front and rear ends of the droplet, D is the channel diameter corresponding to the maximum radial diameter of the droplet, Q_C is the flow rate of the continuous phase, A_{axial} is the axial projection area of the liquid droplet, $\tau(x)$ is the shear rate, directly measured by PIV:

$$\bar{\tau} = \left(\frac{\partial W}{\partial y} + \frac{\partial V}{\partial z}\right)\bar{i} + \left(\frac{\partial U}{\partial z} + \frac{\partial W}{\partial x}\right)\bar{j} + \left(\frac{\partial V}{\partial x} + \frac{\partial U}{\partial y}\right)\bar{k} \#(4)$$

where the formula describes the shear parallel to the yz-, zx- and xy-planes respectively. For planar data, only shear parallel to the xy-plane can be determined:

$$\tau = \frac{\partial V}{\partial x} + \frac{\partial U}{\partial y} \#(5)$$

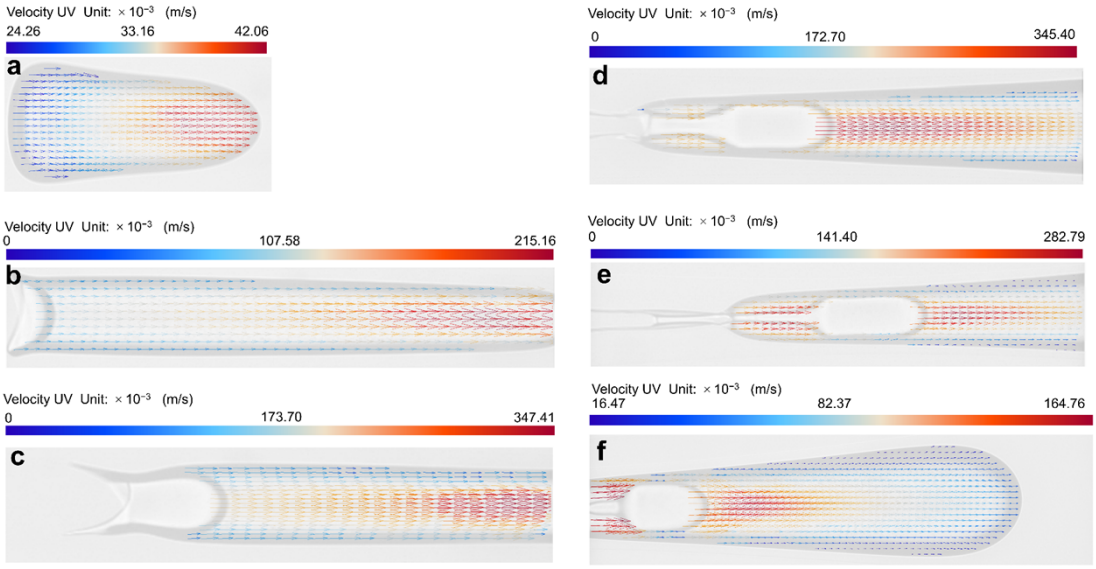

Supplementary Figure S5 (a-f) Velocity vector maps within the droplet at various positions as it passes through the constriction. The flow rate of the continuous phase is 150 μL/min, while the flow rate of the dispersed phase is 20 μL/min.

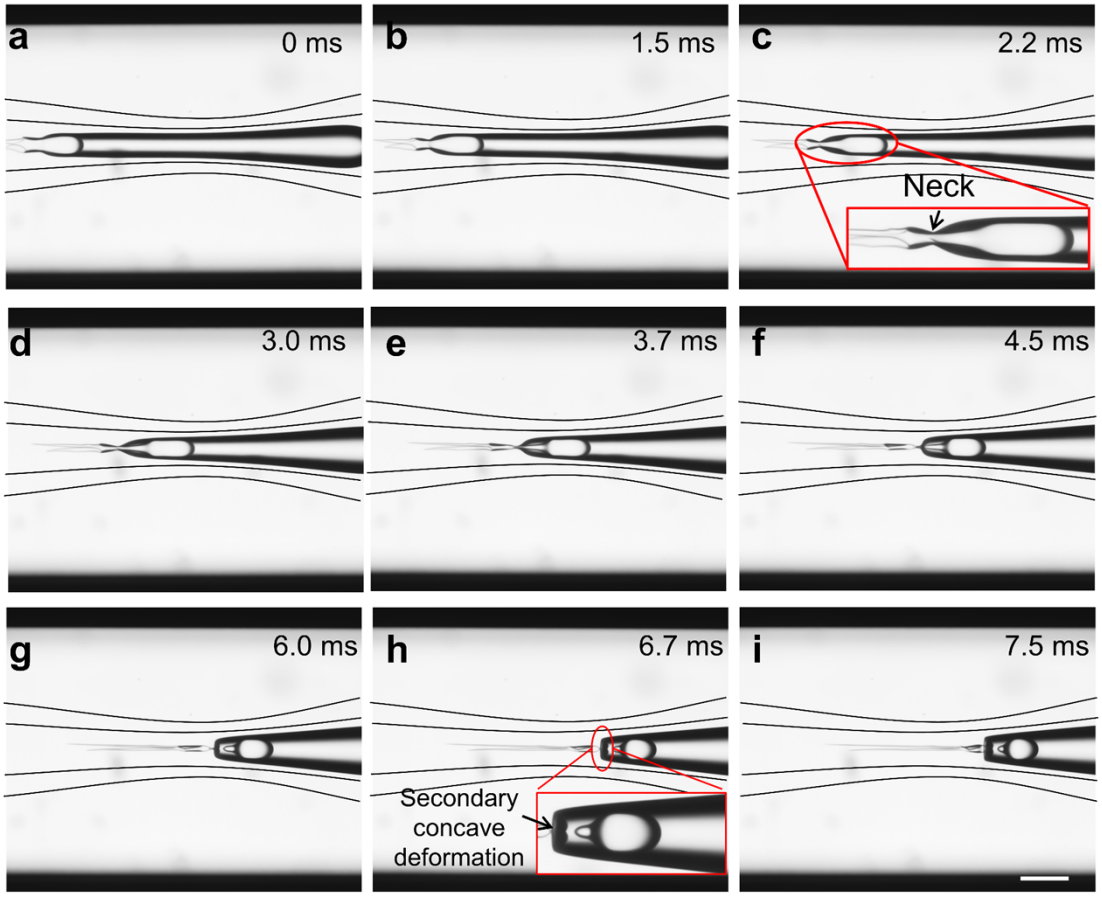

Supplementary Figure S6 As droplets traverse the constriction, microscopic images capture the concave deformation of the droplet tail. Curves are plotted to illustrate both the inner and outer walls of the channel, enhancing clarity in the presentation. (a-c) The droplet tail contracts toward the center due to the channel's confinement, forming a neck. (d-f) The neck gradually tapers. And the engulfed droplet proceeds downstream. (g-i) The neck experiences rupture. The droplet tail undergoes a secondary concave deformation. Scale bar: 200 μm.

4. Conditions for triggering and adjusting drop drinking

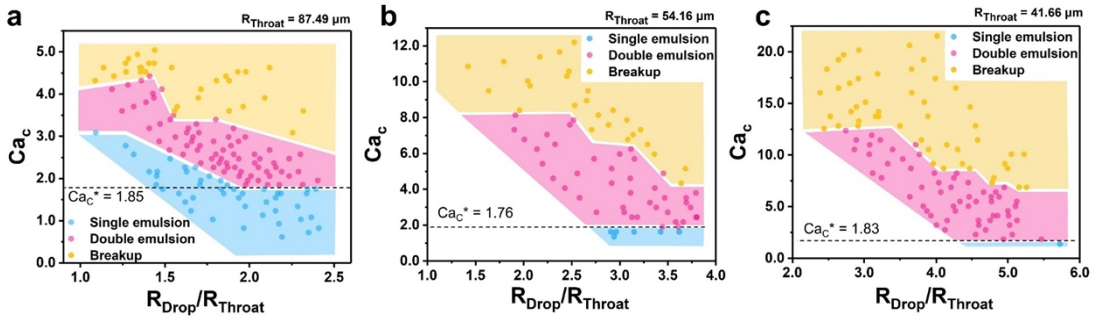

Supplementary Figure S7 The state diagrams illustrate the Ca_c corresponding to three distinct states of the droplet as it traverses the constriction, where the R_{Throat} values are (a) 87.49 μm, (b) 54.16 μm, and (c) 41.66 μm, respectively.

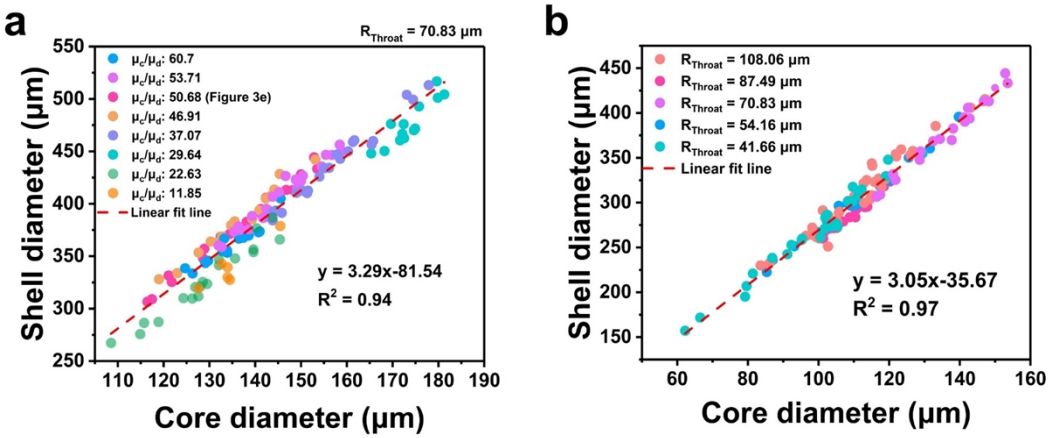

Supplementary Figure S8 (a) Shell diameter of double emulsion as a function of core diameter under different viscosity ratio (μ_c/μ_d) between the continuous phase (μ_c) and the dispersed phase (μ_d). (b) Measurement of shell diameter as a function of core diameter under different capillary systems.

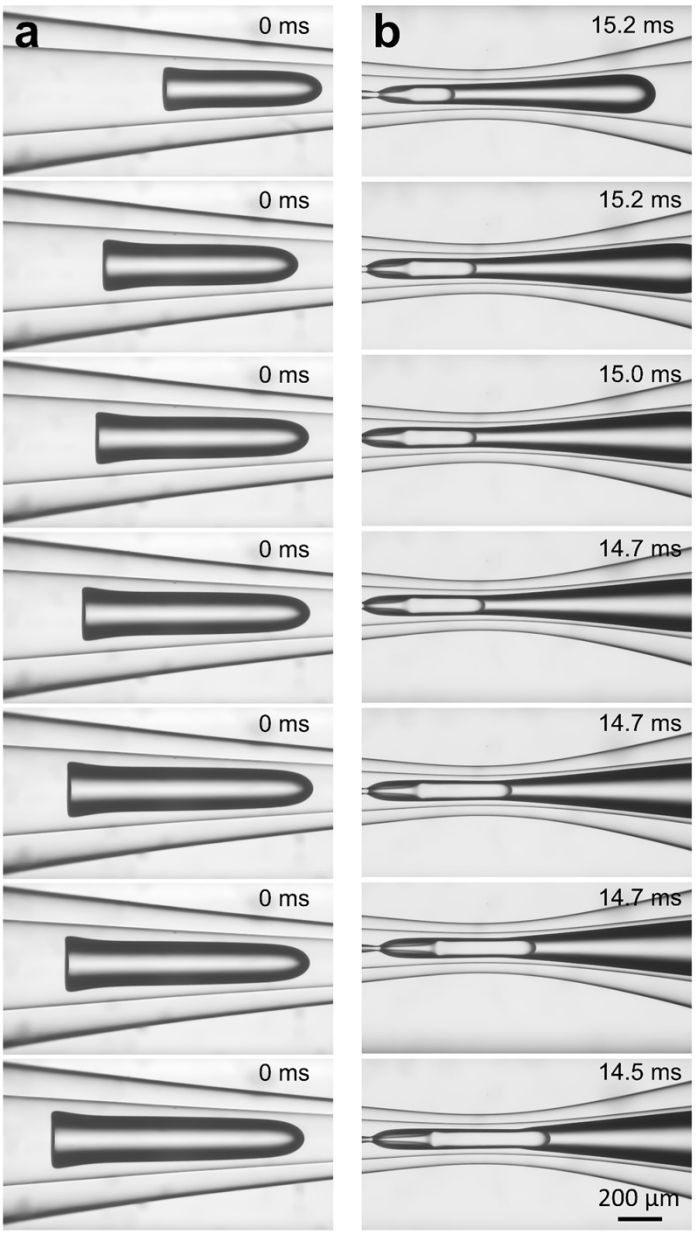

Supplementary Figure S9 As the size of droplets increases, the concave deformation at the tail progressively shifts upstream, leading to a more pronounced engulfment of the continuous-phase liquid. (a) The images illustrate the positions of droplets with varying sizes at the initiation of concave deformation in the upstream region of the constriction. (b) The liquid column formed by the engulfed continuous-phase liquid are depicted as the droplet tail passes through the throat of the constriction.

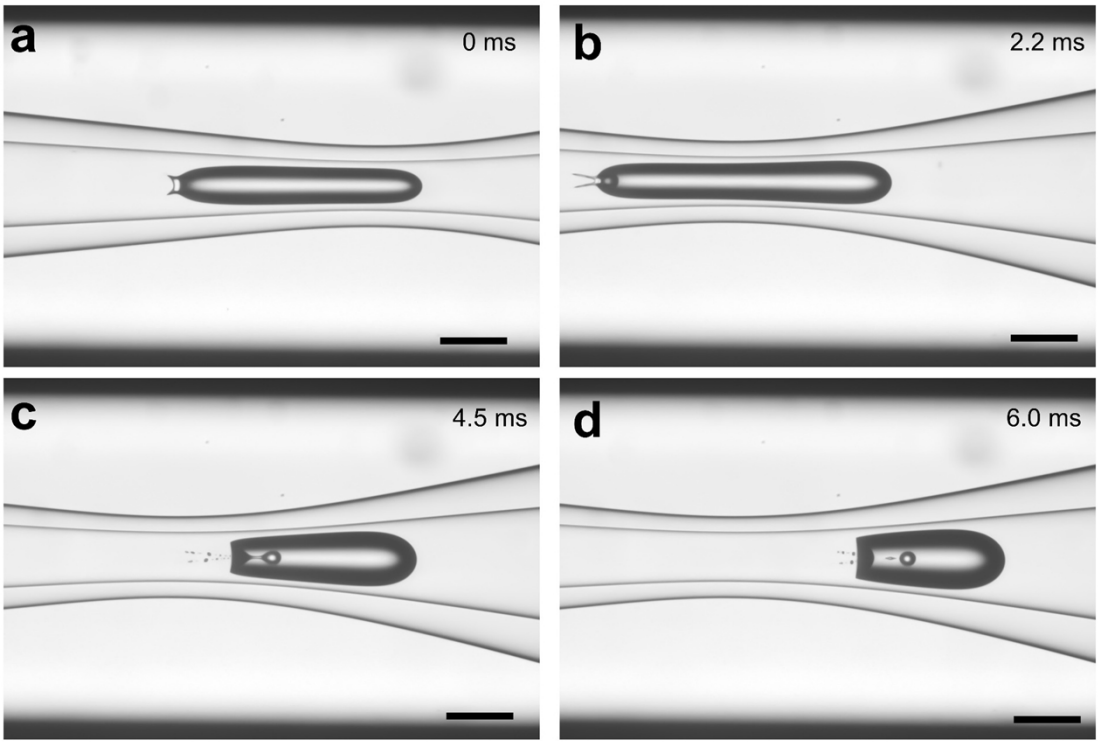

Supplementary Figure S10 (a-d) A series of photos captured by a high-speed camera showing a droplet passing through a constriction with a surface tension of 9.08 mN/m. The liquid system used is no.13 in **Table S2**. Scale bars: 200 μm.

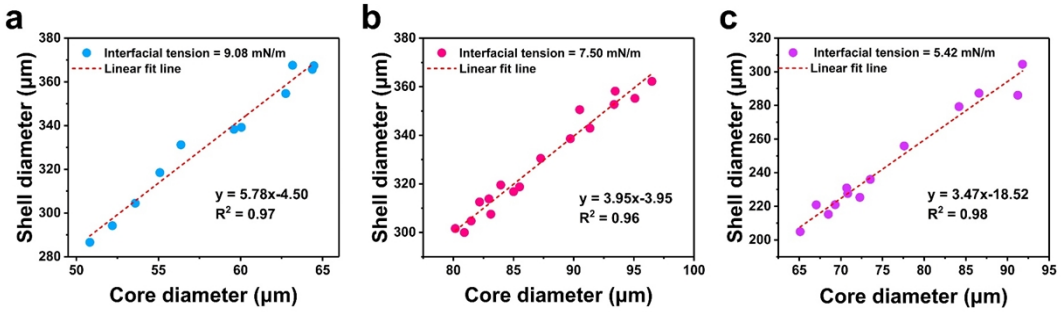

Supplementary Figure S11 Measurement of shell diameter as a function of core diameter. Interfacial tensions between the continuous phase and the liquid droplet phase are (a) 9.08, (b) 7.50, and (c) 5.42 mN/m.

Supplementary Table S2 Physical properties of liquid/liquid system in the experiment at 20℃.

	Continuous oil phase	Dispersed aqueous phase	Aqueous phase viscosity (mPa.s)	Oil phase viscosity (mPa.s)	Interfacial tension γ (mN/m)	Aqueous phase density (g/cm^3)	Oil phase density (g/cm^3)
1	Paraffin	water	1.00*	40.7	32.79	1.00	0.844
2	mine oil (heavy)	water	1.00*	144.3	49.50	1.00	0.862
3	mine oil (light)	water	1.00*	24.28	50.95	1.00	0.838
4	mine oil (light)+5 wt. % EM90	water	1.00*	29.64	3.60	1.00	0.843
5	5 mL mine oil (heavy)+25 mL mine oil (light)+5 wt. % EM90	water	1.00*	37.07	3.69	1.00	0.841
6	4 wt. % EM90 Paraffin	water	1.00*	46.91	3.42	1.00	0.899
7	5 wt. % EM90 Paraffin	water	1.00*	50.68	3.38	1.00	0.899
8	6 wt. % EM90 Paraffin	water	1.00*	53.71	3.29	1.00	0.899
9	8 wt. % EM90 Paraffin	water	1.00*	60.7	3.33	1.00	0.900
10	mine oil (light)+5 wt. % EM90	10 wt.% glycerol	1.50*	29.64	3.25	1.02	0.843
11	mine oil (light)+5 wt. % EM90	30 wt.% glycerol	2.50*	29.64	3.46	1.06	0.843
12	mine oil (light)+5 wt. % EM90	50 wt.% glycerol	6.00*	29.64	4.16	1.12	0.843
13	15 mL mine oil (heavy)+15 mL mine oil (light)	water in 1 wt. % SDS	1.13	49.78	9.08	1.00	0.843
14	Paraffin + 8 wt. % PGPR	water	1.08	55.09	7.50	1.00	0.898
15	15 mL mine oil (heavy)+15 mL mine oil（light）	water in 1 wt. % CTAB	1.23	49.78	5.42	1.00	0.843

*The data of viscosity of water and glycerol aqueous solution is obtained from Segur and Oberstar.[3]

5. Multiple droplet drinking

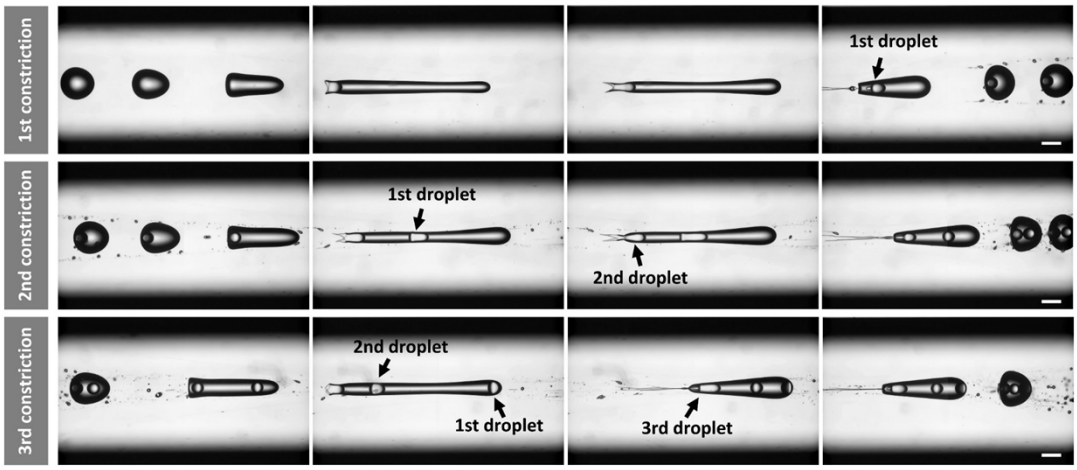

Supplementary Figure S12 After traversing three constrictions, single emulsions experience three consecutive droplet-drinking events, culminating in the formation of triple-core double emulsions, where the number of cores aligns with the number of constrictions. The scale bars represent 200 μm.

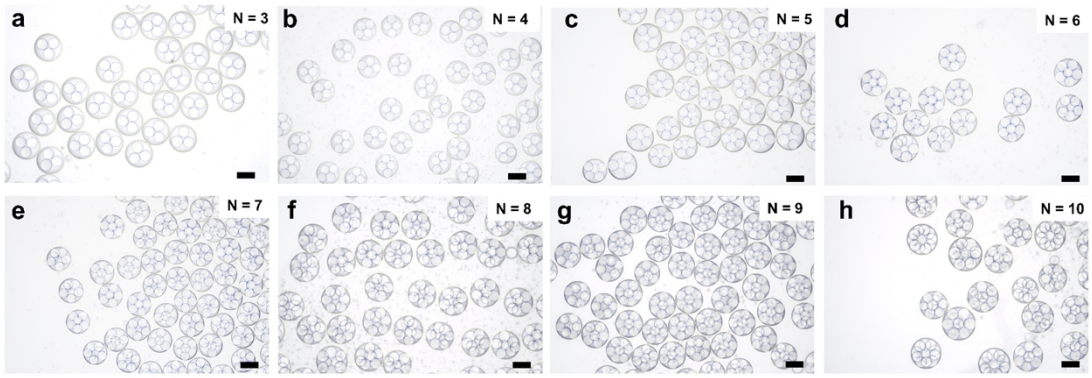

Supplementary Figure S13 O/W-type droplets form multi-core double emulsions The O/W-type droplets are prepared using a water solution containing 5 wt.% Tween 20-surfactant as the outer phase and petroleum ether as the inner phase. When the number of constrictions ranges from 3 to 10, the number of cores equals the number

of constrictions. Scale bars: 200 μm.

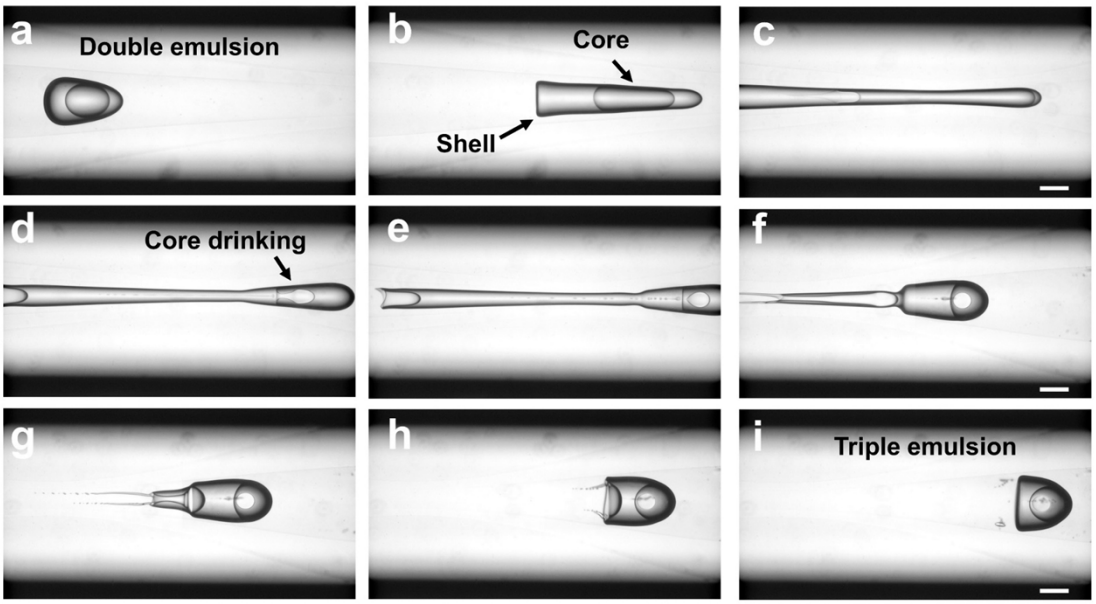

Supplementary Figure S14 (a-i) Microscopic snapshot of a double emulsion undergoing core-drinking behavior, resulting in a tiple emulsion. Scale bars: 200 μm.

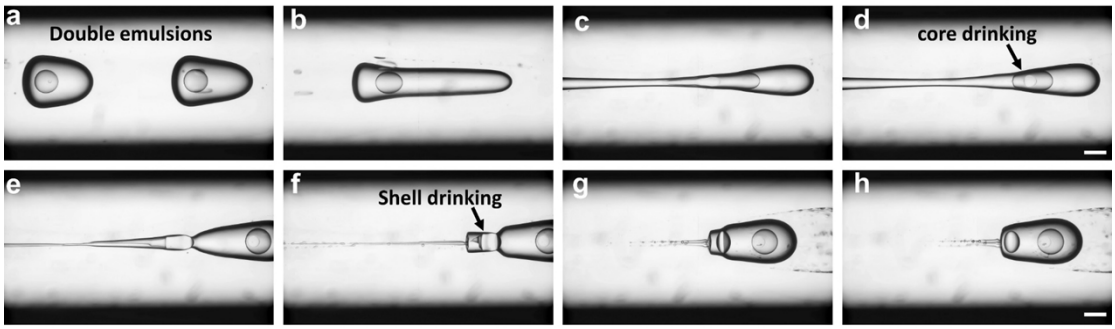

Supplementary Figure S15 (a-h) Microscopic snapshot of double emulsions undergoing simultaneous core-drinking and shell-drinking behaviors. Scale bars: 200 μm.

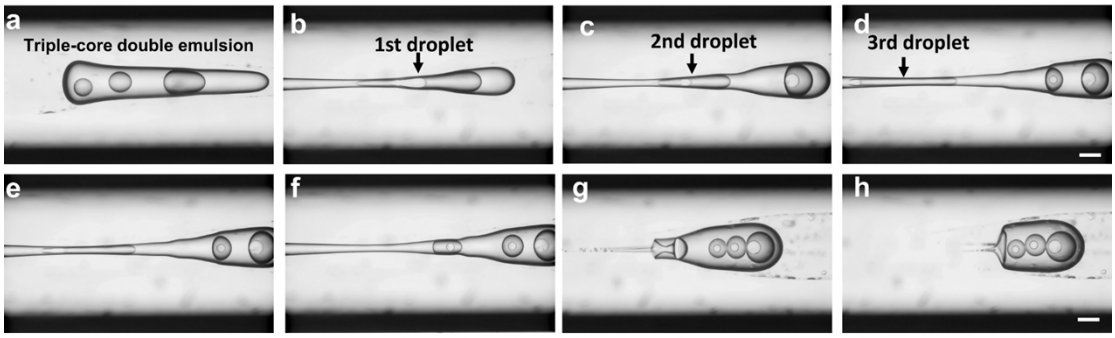

Supplementary Figure S16 (a-h) Microscopic snapshot of a triple-core double emulsion in which core-drinking behaviors occurs sequentially in the three cores after passing through the constriction. Scale bars: 200 μm.

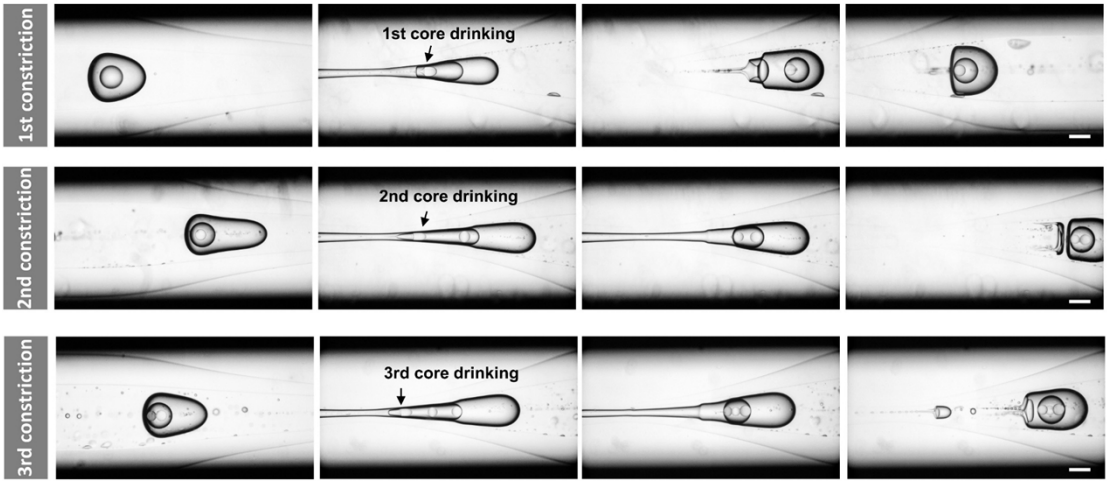

Supplementary Figure S17 After traversing three constrictions, a single-core double emulsion experiences three consecutive core-drinking behaviors, resulting in triple emulsions that contain three droplets in the innermost level. Scale bars: 200 μm.

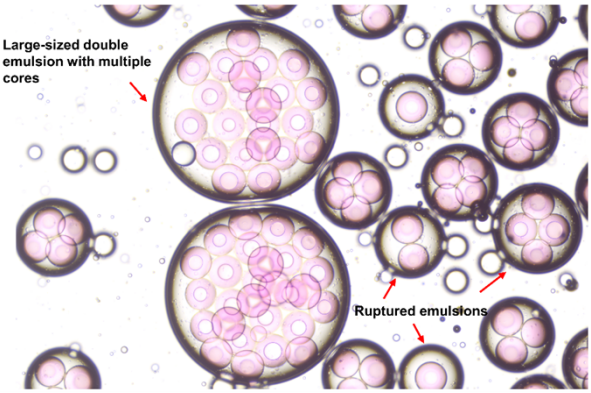

Supplementary Figure S18 Large-sized double emulsions, which encapsulate multiple cores, may undergo rupture while traversing constriction; however, each individual core possesses the capability to undergo core drinking.

6. Droplet-drinking clicking reaction

Due to the presence of saturated surfactants in the outer phase liquid, the engulfed droplets exhibit stability within the double emulsion, while the original HRP-core droplets, not entirely stabilized by EM90-surfactant molecules in the middle phase, show a tendency to fuse.

According to the study of Mazutis and Griffiths,[4,5] the fusion of the two core-droplets is influenced by the coverage Γ of surfactant molecules on the droplet surface which can be described using the Ward and Tordai model:[6]

$$\Gamma(t) = \Gamma(0) + 2\sqrt{\frac{D}{\pi}}\int_0^{\sqrt{t}} \left[c_e - c_s(t-\xi)\right] d(\sqrt{\xi}) \#(6)$$

Where Γ(t) is the interfacial coverage at time t, Γ(0) is initial coverage, D is the diffusion coefficient, c_e is the surfactant concentration in the bulk far from the

interface, c_s is the subsurface concentration and ξ is a variable having value from 0 to time t. When $c_s \ll c_e$, which is typical for microfluidic systems, the above equation can be reduced to:

$$\Gamma(t) = \Gamma(0) + 2c_e\sqrt{\frac{D}{\pi}}\sqrt{t} \#(7)$$

Since $\Gamma(0)$ and D are unknown, interfacial coverage can be determined by applying the nonlinear Langmuir adsorption isotherm in combination with Gibbs equation:

$$\Gamma(t) = \Gamma_\infty\left[1 - exp\left(-\frac{\gamma_0 - \gamma}{RT\Gamma_\infty}\right)\right] \#(8)$$

$$\gamma_e = \gamma_0 - RT\Gamma_\infty ln\left(1 + {}^{c}/_{a_L}\right) \#(9)$$

Γ_∞ is the saturating surfactant concentration at the interface, γ, γ_0 and γ_e are interfacial tensions at time t, at time t = 0 and at equilibrium, respectively. R represents the gas constant, T stands for absolute temperature, and a_L denotes the Langmuir constant. To determine the constant Γ_∞, equilibrium interfacial tension values γ_e obtained from adsorption experiments (**Fig. S19a**) are plotted against the corresponding surfactant concentrations (c) and fitted to equation (9). This results in Γ_∞ = 0.0244 mol/m² and a_L = 0.00171 (mass fraction). The interfacial tension of the droplet produced with 0.1 wt. % EM90-surfactant decreased to 9.55 mN/m at t = 13 s, coinciding with the onset of its merger with the injected droplet. This corresponds to a surface coverage of Γ(13s) = 0.0091 mol/m² or 37.29% of the maximum coverage. Accordingly, droplets produced with 1 wt. % and 0.01 wt. % of the EM90-surfactant had a coverage corresponding to 41.67% (Γ(13 s) = 0.01 mol/m²) and 22.9% (Γ(0 s) =

0.0056 mol/m^2) of maximum adsorption, respectively. At surfactant concentrations of 1 wt. %, little coalescence occurs, whereas at lower concentrations (0.01 wt. %) the double emulsions were unstable and the core droplets of the double emulsion usually break up just as they are created.

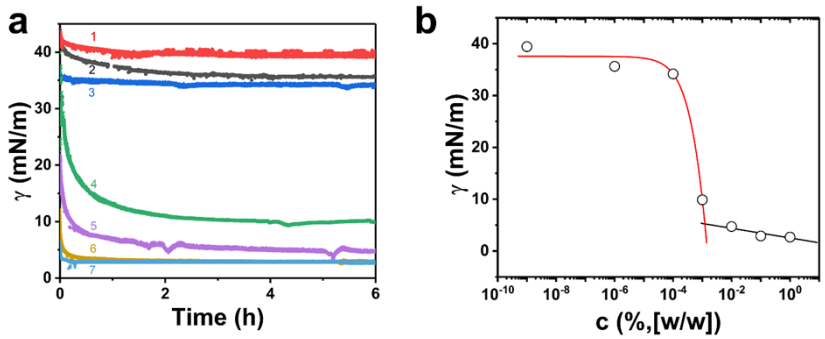

Supplementary Figure S19 Surfactant adsorption analysis using pendant drop method. (a) Dynamic interfacial tension measurements of adsorption of EM90 surfactant onto a water-petroleum ether interface at different surfactant concentrations over 6 hours of incubation. The concentration of surfactant (c) was (1) 10^{-9}, (2) 10^{-6}, (3) 10^{-4}, (4)10^{-3}, (5)10^{-2}, (6) 10^{-1}, (7) 1 % (w/w) of EM90 surfactant. Numbers on the left side of each curve correspond to the list of surfactant concentrations as indicated above. (b) Equilibrium interfacial tension values γ_e for petroleum ether and water interface as a function of EM90 surfactant concentration (c). The red solid line represents a least square curve fit to the Langmuir model. The fit parameters were Γ_∞ = 0.0244 mol/m^2.

7. Reference

1. Stone, H. A. On lubrication flows in geometries with zero local curvature. *Chem. Eng. Sci* **60**, 4838-4845 (2005).
2. Garstecki, P., Fuerstman, M. J., Stone, H. A. & Whitesides, G. M. Formation of droplets and bubbles in a microfluidic T-junction-scaling and mechanism of break-up. *Lab Chip* **6**, 437-446 (2006).
3. Segur, J. B. & Oberstar, H. E. Viscosity of glycerol and its aqueous solutions. *Ind. Eng. Chem.* **43**, 2117-2120 (1951).
4. Mazutis, L. & Griffiths, A. D. Selective droplet coalescence using microfluidic systems. *Lab Chip* **12**, 1800-1806 (2012).
5. Mazutis, L., Baret, J.-C. & Griffiths, A. D. A fast and efficient microfluidic system for highly selective one-to-one droplet fusion. *Lab Chip* **9**, 2665-2672 (2009).
6. Ward, A. F. H. & Tordai, L. Time-dependence of boundary tensions of solutions i. The role of diffusion in time-effects. *J. Chem. Phys.* **14**, 453-461 (2004).